Phase Diagram of $BaTiO_3$

T. Ishidate and S. Abe
Department of Physics, Faculty of Science, Shizuoka University, Shizuoka, Japan

H. Takahashi and N. Môri
The Institute for Solid State Physics, The University of Tokyo, Tokyo, Japan
(Received 1 October 1996)

The temperature-pressure phase diagram of $BaTiO_3$ has been determined by means of a dielectric measurement. All successive phase transition temperatures decrease with increasing pressure with critical index $\phi = 1$, in the classical limit, and $\phi = 2$, in the quantum limit. The dielectric behavior close to the quantum region agrees with the quantum theoretical prediction. In $BaTiO_3$ the crossover region from the classical limit to the quantum one is observed in the range of pressure 4 to 8 GPa and temperature 0 to 200 K. [S0031-9007(97)02793-2]

PACS numbers: 62.50.+p, 81.30.–t

It is well known that $BaTiO_3$ undergoes successive phase transitions from cubic to tetragonal (C-T), tetragonal to orthorhombic (T-O), and orthorhombic to rhombohedral ($O-R$), which are satisfactorily interpreted within the classical framework of the Landau-Devonshire theory [1]. The Curie-Weiss law, characteristic of the paraelectric-ferroelectric phase transition, reduces to the soft mode theory through the Lyddane-Sachs-Teller relation [2]. However, at the transition temperature T_c near 0 K, the lattice vibrational mode would be influenced by quantum fluctuation such as zero point vibration. The quantum theoretical treatment predicts

$$T_c(S) \propto (S_c - S)^{1/\phi}, \tag{1}$$

with the critical exponent $\phi = 2$ close to the quantum limit. Here, S is an interaction parameter and S_c is its value at $T_c = 0$ [3,4]. The interaction parameter S is an external parameter such as pressure or chemical composition which controls the interaction [5,6].

The study of the dielectric property of $BaTiO_3$ under high pressure was performed by Samara [7]. He found that the C-T phase transition temperature $T_{C\text{-}T}$ decreased linearly with pressure in the range from 1 bar to 3 GPa. It corresponds just to the classical limit of the critical exponent $\phi = 1$ in Eq. (1). Samara suggested the existence of the critical point, which implies the crossing of the first- and second-order phase transitions, at a pressure higher than 3 GPa. The elastic property of $BaTiO_3$ under high pressure was studied at room temperature by Ishidate and Sasaki [8]. They found an elastic anomaly in the cubic phase near the C-T transition and interpreted that the elastic anomaly was caused by the anisotropy field. The decrease of the elastic anomaly under high pressure rather than the atmospheric pressure also supported that the first-order phase transition was going toward the second-order one. The existence of the critical point ($p = 3.5$ GPa and $T = -40$ °C) was confirmed by Decker and Zhao [9].

Although the phase transition in $BaTiO_3$ has been extensively studied [2,10], the systematic investigation of the temperature-pressure phase diagram has not been performed because of the difficulty of high pressure experiments. The recent development of high pressure apparatus enabled one to do the electric measurement at high pressure up to 10 GPa and low temperature down to 4 K continuously [11].

The purpose of this paper is to determine the temperature-pressure phase diagram of $BaTiO_3$ and to make clear the dielectric behavior of $BaTiO_3$ in the quantum limit.

The b-cut plate was prepared from a melt-grown $BaTiO_3$ single crystal (NEC Co. Ltd.) which has the transition temperature 127 °C. Au paste was painted on both planes of the sample (typically $0.9 \times 0.6 \times 0.03$ mm^3 in size), and Au wire (0.02 mm diam) was used as a lead. The sample was set in a teflon capsule together with flourinert oil (FC-70), used as a pressure transmitting medium. The teflon capsule was placed in the center of a pyrophilite cube of $6 \times 6 \times 6$ mm^3 in size, used as a gasket material. The Au wire was fixed on the surfaces of the pyrophilite cube through the interior and was connected with the external leads through contact with two metallic anvils. The pyrophilite cube was placed in a cubic anvil apparatus which could generate the pressure up to 8 GPa. The details of the apparatus have already been described elsewhere [11]. Temperature was measured using a Pt-Co resistance thermometer attached to the anvil. The capacitance for 1, 10, and 100 kHz frequencies, as a function of temperature from 50 or 80 K to 300 K, was measured by a *LCR* meter (HP 4274A) at a heating rate of about 0.3 K/min under constant pressure. In this experiment, a large part of the stray capacitance might have been arising from among the six anvils, two of which played effective roles as electrodes. The net capacitance of the sample C_{samp} can be related to the observed one C_{obs} as follows:

$$1/C_{\text{obs}} = 1/(C_{\text{samp}} + C_A) + 1/C_B, \tag{2}$$

 © 1997 The American Physical Society

where C_A and C_B are stray capacitances, contributing in parallel and series, respectively. The capacitance C_A is that induced between the anvils, and C_B is that induced between the anvil and electrode lead. In order to deduce C_{samp} from C_{obs}, the pressure dependence of the capacitance at room temperature was measured continuously. The pressure dependence of C_{samp} was fitted to the Curie-Weiss law with respect to pressure, $C_{\text{samp}} = C^*/(p - p_c)$, after Samara [7], where C^* is the Curie constant, dependent on the temperature. The fitting was satisfactorily performed in the high dielectric region over pressure 2.3 to 5 GPa but showed a slight deviation above 5 GPa. This deviation might have been caused by the increase of nonhydrostaticity due to solidification of the pressure transmitting medium under pressure higher than 5 GPa. However, further correction to the stray capacitance above 5 GPa was not made. As a result, the contribution of C_B to C_{obs} was less than 1% but that of C_A varied from 5% to 70%, depending on the sample setting. Thus, the contribution to C_{obs} came mainly from the parallel stray capacitance C_A, which was specified by the electrode structure. For data analysis the temperature dependence of C_A and C_B was neglected.

The transition temperature was determined from the position of the dielectric peak. For the paraelectric-ferroelectric C-T transition the dielectric anomaly is very large, but for the ferroelectric-ferroelectric T-O and O-R transitions, it is very small. In order to confirm the peak position of the latter transitions, we measured the strain change of the ceramic disk sample (0.7 mm thickness and 8 mm diam) using a strain gauge with a piston-cylinder-type pressure apparatus which can generate the pressure up to 2 GPa. The temperature, at which the strain anomaly was observed, corresponded to that of the dielectric peak. The phase diagram of $BaTiO_3$ was determined as shown in Fig. 1.

First, the transition temperatures $T_{C\text{-}T}, T_{T\text{-}O}$, and $T_{O\text{-}R}$ decrease linearly with increasing pressure up to 3 GPa with the respective initial slope $dT_c/dp = -55, -28$, and -13.5 K/GPa, in agreement with Samara's result [7,12]; $-55, -29$, and 12.3 K/GPa, following Eq. (1) in the classical limit.

Above 4 GPa they decrease rather steeply, but each phase exists stably even in the vicinity of $T = 0$. To ensure Eq. (1), $T^2_{C\text{-}T}, T^2_{T\text{-}O}$, and $T^2_{O\text{-}R}$ are plotted as a function of pressure in Fig. 2. It is clear that they are all changing linearly with pressure above 4 GPa. The values of the respective critical pressure, i.e., the transition pressure at $T_c = 0$, are 6.5, 6.0, and 5.4 GPa. These characteristic behaviors are in agreement with Eq. (1), in the quantum limit. Note that the pressure dependence of each transition temperature in $BaTiO_3$ obeys Eq. (1) even at 200 K although the quantum effect is expected at very low temperature. For $T_{T\text{-}O}$, Eq. (1) holds entirely over the observed temperature-pressure range, but in the case of $T_{O\text{-}R}$, it is exceptional for temperature near 200 K and pressures lower than 2 GPa. In this respect, it is noted that the O-R transition exhibits especially strong hysteresis [12].

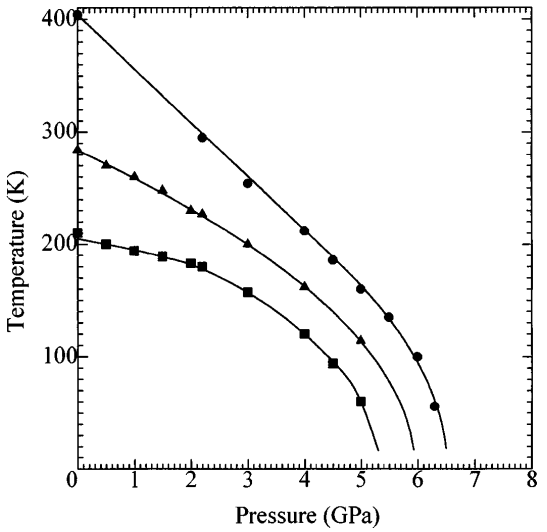

FIG. 1. Phase diagram of $BaTiO_3$. The solid lines are guide to eyes.

Recently, the phase diagram of the hexagonal-orthorhombic phase transition in hexagonal $BaTiO_3$ (h-$BaTiO_3$), which is caused by the softening of the silent mode, has been measured by Akishige *et al.* [13]. Their result showed that the critical pressure was 3.4 GPa in h-$BaTiO_3$, and the pressure dependence of the transition temperature obeyed Eq. (1) with $\phi = 2$ over the entire temperature region of 0 to 222 K. In comparison with the present result for perovskite $BaTiO_3$ (p-$BaTiO_3$), it seems to be reasonable since the specific heat of h-$BaTiO_3$

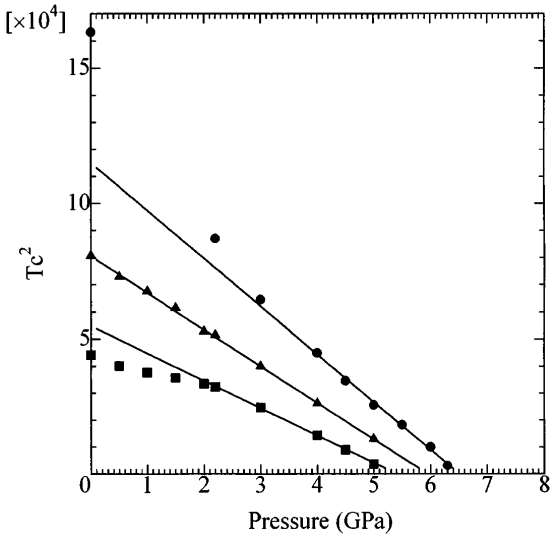

FIG. 2. The squares of the transition temperatures vs pressure. Above 4 GPa, the critical index in Eq. (1), $\phi = 2$. The values of the critical pressure at $T_c = 0$ for $T_{C\text{-}T}, T_{T\text{-}O}$, and $T_{O\text{-}R}$ are $p_c = 6.5, 6.0$, and 5.4 GPa, respectively.

shows a similar behavior to that of p-$BaTiO_3$ to yield a similar Debye temperature [14].

We are concerned with the critical exponent of the dielectric constant at the C-T phase transition, close to the quantum limit $p_c = 6.5$ GPa. The log-log plot of the inverse dielectric constant χ vs the temperature difference $\Delta T = T - T_c$ is shown in Figs. 3(a) and 3(b) for 4 and 7 GPa, respectively.

The slope obtained from the plots gives the critical index γ_T in the following expression:

$$\chi = b\,(T - T_c)^{\gamma_T}, \tag{3}$$

with some constant b. Here, $\gamma_T = 1$ in the classical limit and $\gamma_T = 2$ in the quantum limit. The pressure dependence of γ_T is shown in Fig. 4. While at 3 GPa, $\gamma_T = 1$ and it still belongs to the classical region; the value of γ_T increases with pressure until it reaches near the critical pressure $p_c = 6.5$ GPa and then decreases. It should be noted that γ_T started to deviate from the classical value near 4 GPa, where T_C^2 varied linearly with pressure, as shown in Fig. 2.

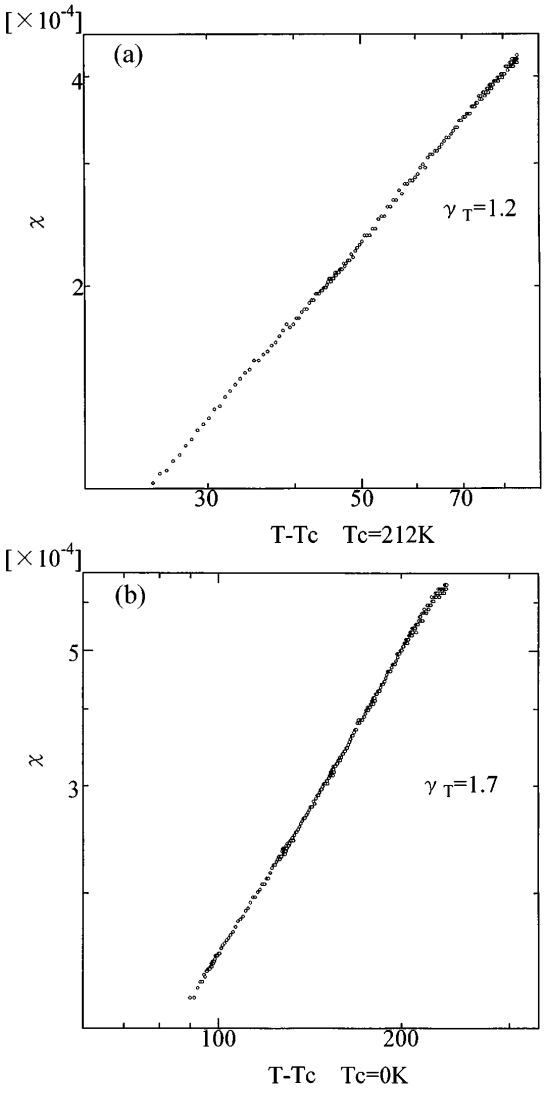

FIG. 3. The log-log plot of the inverse dielectric constant χ vs the temperature difference $\Delta T = T - T_c$, at (a) 4 GPa and (b) 7 GPa. The slope gives the critical index in Eq. (3), $\gamma_T = 1.2$ and $\gamma_T = 1.7$ for (a) and (b), respectively. The dielectric peak in the vicinity of T_c is rounded [which is not shown in (a)] because a relatively large field strength (about 1 kV/cm) was applied. (b) This shows the dielectric measurement from 80 K.

The highest value of γ_T is observed to be 1.7, which is lower than the predicted value of 2.0. This might have been caused by a slight increase of C_A above 5 GPa, as mentioned earlier. However, the present result is in agreement with the prediction from quantum theory. The crossover region from $\gamma_T = 1$ to $\gamma_T = 2$ is observed over the pressure range from 4 to 8 GPa.

The pressure dependence of χ at constant temperature can be represented by the following expression similar to Eq. (3):

$$\chi = d(p - p_c)^{\gamma_p}, \tag{4}$$

with some constant d. The quantum theory predicts $\gamma_p = \gamma_T/\phi = 1$ at $T_c = 0$. Thus the pressure dependence of χ in the quantum limit is the same as given by the Curie-Weiss law in the classical limit.

Consequently, Eq. (4) should hold over the entire temperature region. The pressure dependence of χ at 200 and 100 K is shown in Fig. 5. Both the cases seem to obey Eq. (4). The slope of the line at 200 K is larger than that at 100 K. This implies that the Curie constant C^* $(= 1/d)$ decreases with increasing temperature, in agreement with Samara's result [7]. But note that χ at 100 K is not exactly zero at the transition point. This disagreement might have been coming from the increase of the stray capacitance above 5 GPa and negligence of

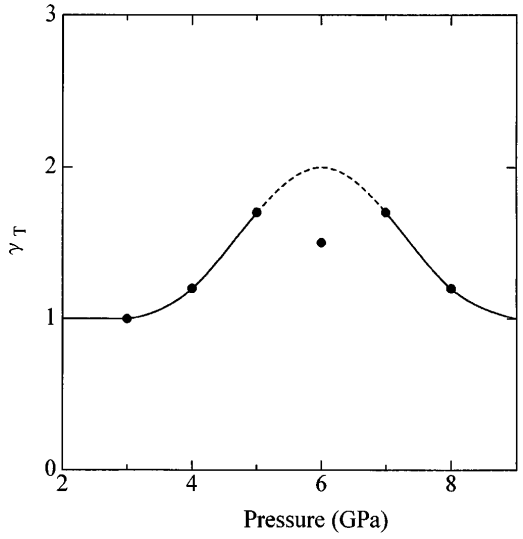

FIG. 4. The critical index γ_T vs pressure. At 3 GPa, $\gamma_T = 1$, and it belongs to the classical region. Above 4 GPa, γ_T increases with pressure up to the critical pressure $p_c = 6.5$ GPa and then decreases again toward the classical limit. The solid line is guide to eyes.

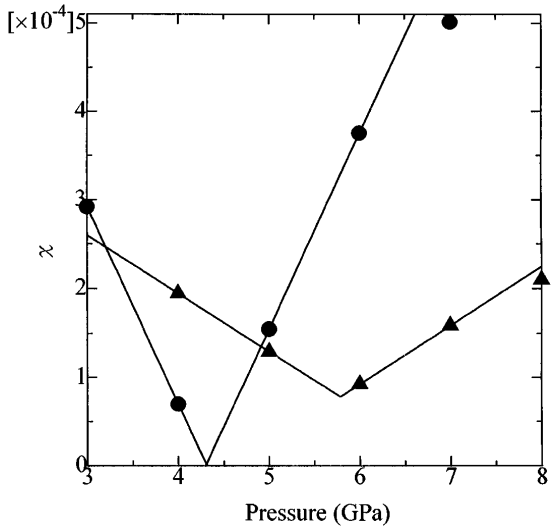

FIG. 5. The inverse dielectric constant χ vs pressure at 200 K (circle) and 100 K (triangle), respectively. The critical index $\gamma_p = 1$ holds in the cubic phase.

the temperature dependence of the stray capacitance. As seen from Fig. 3(b), the influence of the latter would be less than that of the former.

In many perovskite-type ferroelectrics the phase diagram has been extensively studied in the mixed system as a function of the composition [10]. The phase diagram of $BaTiO_3$ shown in Fig. 1 closely resembles that of $Ba_{1-x}Sr_xTiO_3$ (BST). In BST the lattice parameter decreases with the increase of x, the successive phase transition persists up to the value $x = 0.7$, and the cubic to tetragonal phase transition occurs even extremely close to the value $x = 1.0$. In the mixed system which obeys Vegard's law, the lattice contraction due to the mixing effect can be compared with that due to the pressure effect.

For example, for $x = 0.3$ in BST, the ferroelectric phase transition occurs at room temperature, and the lattice contraction is 0.03 Å compared to that for $x = 0$. On the other hand, the phase transition pressure p_c of $BaTiO_3$ is 2.3 GPa at the room temperature. The estimation of the lattice contraction by using the bulk modulas $B = 130$ GPa at normal pressure [8] gives 0.023 Å. This value is very close to that of BST. Thus the Sr-doping effect in $BaTiO_3$ plays an equivalent role to the pressure effect with respect to the lattice contraction. However, in BST the value of the interaction parameter S_c at $T_c = 0$ has not been confirmed.

Recently, the phase diagram of $BaTiO_3$ was theoretically derived from the first principle on the basis of a density functional method by Zhong, Vanderbilt, and Rabe [15]. Their result shows that the cubic, tetragonal, orthorhombic, and rhombohedral phases exist stably over the entire region and all of the phase lines decrease linearly with increasing pressure, accompanied with the decrease of the tetragonal and orthorhombic regions. The critical pressure was calculated to be $p_c = 13.2$ GPa, which is remarkably higher than the observed value $p_c = 6.5$ GPa. Further, the calculated values of dT_c/dp were -28, -22, and -15 K/GPa for the C-T, T-O, and O-R transitions, respectively, and the value for the C-T transition is especially lower than the observed one. Thus, their result is qualitatively in agreement with the present result, but not quantitatively. Whether the cause of the quantitative difference is due to the lattice error in the local density approximation as they stated, is not clear. However, it would be necessary to recalculate the phase diagram of $BaTiO_3$, taking account of the effect of zero-point vibration.

The authors are grateful to the Murata Electric Co. for kindly supplying the ceramic sample. This work was partially supported by a Grant-in-Aid for Scientific Research from the Ministry of Education, Science and Culture, and also by the Iketani Science and Technology Foundation.

[1] F. Jona and G. Shirane, *Ferroelectric Crystals* (Pergamon, New York, 1962).
[2] M. E. Lines and A. M. Glass, *Principles and Applications of Ferroelectrics and Related Materials* (Oxford University Press, Oxford, 1979).
[3] T. Shneider, H. Beck, and E. Stoll, Phy. Rev. B **13**, 1123 (1976).
[4] R. Morf, T. Shneider, and E. Stoll, Phys. Rev. B **16**, 462 (1977).
[5] G. A. Samara, Physica (Amsterdam) **120B**, 179 (1988), and references therein.
[6] U. T. Hoechli, Ferroelectrics **35**, 17 (1981).
[7] G. A. Samara, Phys. Rev. **151**, 378 (1966).
[8] T. Ishidate and S. Sasaki, Phys. Rev. Lett. **62**, 67 (1989).
[9] D. L. Decker and Y. X. Zhao, Phys. Rev. B **39**, 2432 (1989).
[10] *Ferroelectrics: Oxides* Landolt-Boernstein New Series 111/16a (Springer-Verlag, Berlin, 1981), and reference therein.
[11] N. Môri and H. Takahashi, Pressure Eng. **28**, 124 (1990).
[12] G. A. Samara, Ferroelectrics **2**, 277 (1971).
[13] Y. Akishige, H. Takahashi, N. Môri, and E. Sawaguchi, J. Phys. Soc. Jpn. **63**, 1590 (1994).
[14] Y. Akishige, T. Atake, Y. Saitoh, and E. Sawaguchi, J. Phys. Soc. Jpn. **57**, 718 (1988).
[15] W. Zhong, D. Vanderbilt, and K. M. Rabe, Phys. Rev. B **52**, 6301 (1995).